and

$$v=4\omega L(u)\,u^*/r \tag{17}$$

Equations (5-8) may be easily changed so that derivatives are taken with respect to time instead of E. From Eqs. (4) and (9), it follows that

$$\dot{E}=2\omega/r \tag{18}$$

and the time derivative of any element f can be written

$$\dot{f}=f^*\dot{E} \tag{19}$$

but a way of calculating E as a function of time must be provided. Equation (18) provides the answer. Equation (18) is equivalent to

$$t^*=r/2\omega \tag{20}$$

where

$$r=u\cdot u \tag{21}$$

as follows from Eqs. (2) and (3). From Eqs. (14, 20, and 21) it follows

$$t^*=\frac{1}{2\omega}\left(\frac{\alpha^2+\beta^2}{2}+\frac{\alpha^2-\beta^2}{2}\cos E+\alpha\cdot\beta\sin E\right) \tag{22}$$

Solving Eq. (22) by variation of parameters yields

$$t=t_0+\frac{1}{2\omega}\left[\frac{\alpha^2+\beta^2}{2}E+\frac{\alpha^2-\beta^2}{2}\sin E+\alpha\cdot\beta(1-\cos E)\right] \tag{23}$$

where t_0 is a new element which may be called the initial time element. Equation (23) is essentially Kepler's equation, although the elements which appear in the equation are not identically Keplerian except in the absence of a perturbing potential.

In order that Eqs. (22) and (23) be simultaneously satisfied, the initial time must have a derivative given by

$$t_0^*=(t-t_0)\frac{\omega^*}{\omega}-\frac{1}{2\omega}\left[\alpha\cdot\alpha^*(E+\sin E)+\beta\cdot\beta^*(E-\sin E)+(\alpha^*\cdot\beta+\alpha\cdot\beta^*)(1-\cos E)\right] \tag{24}$$

Equations (5, 7, 8, and 24) can be expressed as derivatives with respect to time simply by multiplying each equation by $\dot{E}$. The result is

$$\dot{\omega}=Q\dot{E} \tag{25}$$

$$\dot{\alpha}=S\dot{E}\sin(E/2) \tag{26}$$

$$\dot{\beta}=-S\dot{E}\cos(E/2) \tag{27}$$

$$\dot{t_0}=(t-t_0)\frac{\dot{\omega}}{\omega}-\frac{1}{2\omega}\left[\alpha\cdot\dot{\alpha}(E+\sin E)+\beta\cdot\dot{\beta}(E-\sin E)+(\dot{\alpha}\cdot\beta+\alpha\cdot\dot{\beta})(1-\cos E)\right] \tag{28}$$

where

$$Q\dot{E}=-\frac{1}{4\omega}\frac{\partial V}{\partial t}-\frac{1}{r}u^*\cdot L^T P \tag{29}$$

$$S\dot{E}=\frac{1}{\omega r}\left[\frac{V}{2}\mu+\frac{r}{4}\left(\frac{\partial V}{\partial u}-2L^T P\right)\right]+\frac{2}{\omega}\dot{\omega}u^* \tag{30}$$

The differential equations of the KS elements are now written in terms of derivatives with respect to time and may be integrated using standard techniques. Kepler's equation [Eq. (23)] is solved at each integration step to obtain the value of E corresponding to the specified time, t.

A price is paid for writing the differential equations as functions of time, however. The time step is no longer internally controlled by the regularization, but must be externally controlled. The original set of equations could integrate through collisions, (r very small) but the appearance of terms proportional to $1/r$ precludes this with the new set. Even in this "deregularized" form, however, the KS method still provides a more stable set of equations than a variation of parameters technique based on Keplerian elements. Computer experiments have verified that the non-Keplerian elements of KS are more slowly varying than Keplerian elements and that feature is preserved in the time dependent set.

References

[1] Pines, S., "Variation of Parameters for Elliptic and Near Circular Orbits," *Astronomical Journal*, Vol. 66, Jan. 1961, pp. 5-7.

[2] Stiefel, E. L. and Scheifele, G., *Linear and Regular Celestial Mechanics*, Springer-Verlag, New York, 1971., pp. 83-92.

Gravitationally Stabilized Satellite Solar Power Station in Orbit

V.A. Chobotov*
The Aerospace Corporation, El Segundo, Calif.

I. Introduction

THE possibility of collecting large amounts of solar energy in space has been studied for a number of years.[1,2] The principal advantage of such schemes is the availability of practically inexhaustable amounts of energy which can be harnessed away from the Earth's active environment. Large structures can be constructed and placed in the synchronous equatorial orbit to collect and transmit solar energy (via microwave) to selected locations on the Earth. No energy storage devices to compensate for the day-night cycles or cloundy weather are required. It is estimated that a 5×12 km solar array can, for example, deliver 5000 MW of power on the ground, assuming a solar array efficiency of 11.3%.[3]

The present study examines an alternative approach employing a larger number of smaller solar collectors attached to a gravitationally stabilized cable in orbit. The problems associated with the construction and active attitude control of very large structures are thus alleviated. A schematic drawing of this concept is shown in Fig. 1 for a 5-GW solar photovoltaic system consisting of fifty-two 750×1500-m panels attached to a 57.75 km tapered cable with a 0.83-km-diam microwave (S-band, 2.45 GHz) transmitting antenna. The total solar array area is 58.5 km^2. The total mass has been estimated to be on the order of 18×10^6 kg. The slipring-connected solar segments are assumed actively controlled within a few degrees to the sun while the long axis of the array is Earth-pointing. A roll oscillation (about the satellite orbital velocity vector) is induced to prevent mutual shadowing of the solar segments when the sun is directly above the array.

The microwave antenna can be steered electronically with a scan angle capability of up to 60 deg thus requiring little or no active attitude control. The accuracy of pointing can be determined to 0.12 mrad. The elimination of sliprings and

Received Oct. 15, 1976; revision received Dec. 22, 1976.

Index categories: Spacecraft Electric Power Systems; Earth Satellite Systems, Unmanned; Spacecraft Attitude, Dynamics, and Control.

*Staff Engineer, Mission Analysis Department, Guidance and Control Division. Member AIAA.

gimbals may also be achieved should a spherical rather than a rectangular array be employed. A tradeoff between design simplicity and efficiency may thus be obtained.

II. Roll Oscillation Requirements

At the vernal and autumnal equinoxes the sun vector is along the local vertical of the satellite twice per day in a synchronous equatorial orbit. The shading of all segments of the array can be minimized or avoided if the cable is then inclined to the local vertical. The required inclination depends on the size, shape, and spacing of the array segments. Since the natural roll frequency of a gravitationally stabilized cable in orbit is nominally equal to twice the orbital angular rate, the angular offset to the local vertical and proper phasing with respect to the sun can be obtained.

For a maximum roll angle $\theta_{rm} = 30$ or 45 deg and the spacing-to-width ratio (h/w) of the segments along the array of either 1, 1.5, or 2, the percent of illumination as a function of satellite orbital position μ, relative to the sun vector at the equinoxes, is as shown in Fig. 2. The results show that for $\theta_{rm} = 30$ deg and $h/w = 1.5$ the maximum shading is about 25% at local noon. This can be further reduced or eliminated entirely by increasing h/w or θ_{rm}. An increase in h/w, however, increases the length of the cable and the power losses. Cable tension and the gravitational restoring torques are also increased. An optimum configuration (with respect to size, shape, and mass) can thus be found. However, large roll oscillations (>20 deg) couple nonlinearly with pitch motions (in the plane of the orbit).[4] Little or no roll oscillations are required at other times of the year.

III. Tension and Restoring Torques

Maximum gravitationally induced tension T_m in the array is at the system center of gravity. For a cable of length L, mass

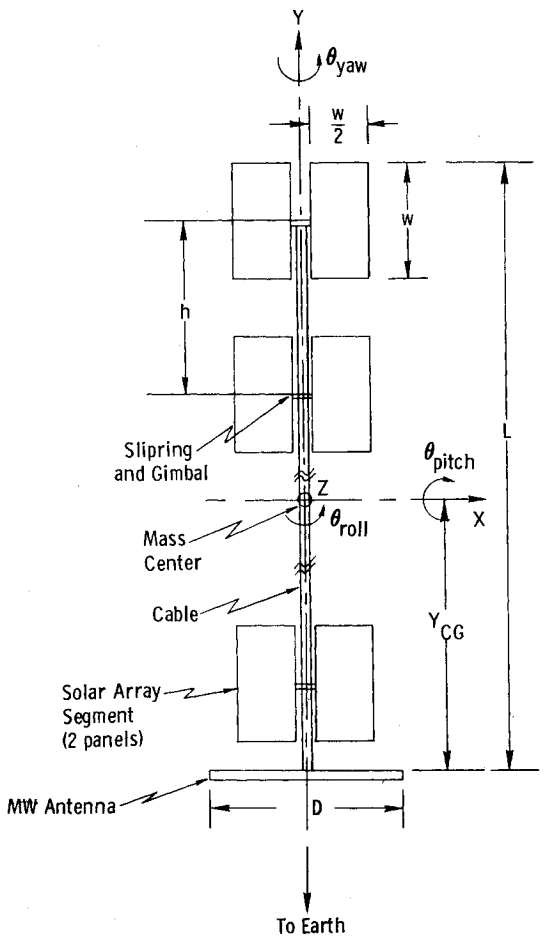

Fig. 1 Gravity-gradient-stabilized satellite solar power station.

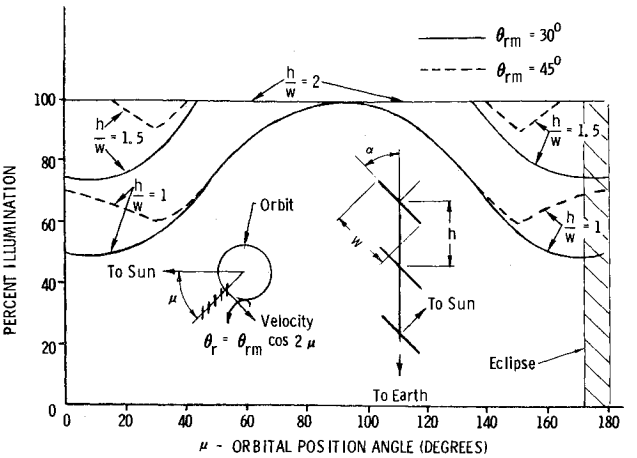

Fig. 2 Percent illumination at equinox.

density σ (with arrays included), and the tip mass M_{ant} of the Earth-pointing antenna

$$T_m = 1.5\omega_0^2 (LM_{ant} + \sigma L^2/4) \quad (1)$$

where ω_0 is the orbital angular rate. For example, if the mass properties for a 5 and 10 GW array are as shown in Table 1, then T_m and the array restoring torques about the pitch, roll and yaw axes are as shown in Table 2. The results show a significant tension when the cable is aligned along the local vertical. As the roll angle increases, however, the tension decreases. This relationship is shown in Fig. 3 where the array tip acceleration ratio T for a dumbbell

$$T = (\dot{\theta}_r/\omega_0)^2 + 3 - 4\sin^2\theta_{rm} \quad (2)$$

is plotted as a function of the maximum roll angle θ_{rm}. For zero roll rate $\dot{\theta}_r = 0$, the maximum value of T (corresponding

Table 1 Area and mass properties

Power output	5 GW	10 GW
MW antenna		
Diameter D, km	0.83	1.18
Mass, 10^6 kg	5.55	10.74
Solar array		
Number of segments (2 panels each)	26	53
Panel size, m^2	750×1500	750×1500
Segment mass, 10^6kg	0.474	0.474
h/w	1.5	1.5
Cable		
Length L, km	57.75	117
Mass, 10^6kg	0.170	0.342
Y_{CG}, km	20.2	41.0
System		
Area, km^2	58.5	117
Inertia, 10^{12}kg-m^2		
I_x	6792	54208
I_y	2.88	6.67
I_z	6795	54213
Mass, 10^6kg	18	36

Table 2 Gravity-gradient tension and restoring torques

	5 GW array	10 GW array
Maximum tension, N (lb)	3467 (780)	15800 (3555)
Pitch restoring torque, N-m/deg	1.89×10^6	15.1×10^6
Roll restoring torque, N-m/deg	2.52×10^6	20.1×10^6
Yaw restoring torque, N-m/deg	251	627

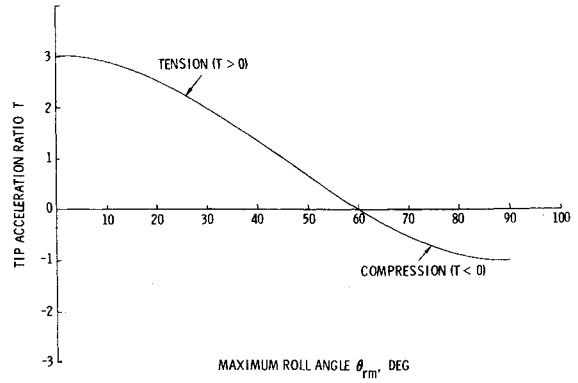

Fig. 3 Tip acceleration ratio T vs maximum roll angle θ_{rm} for a dumbbell in circular orbit.

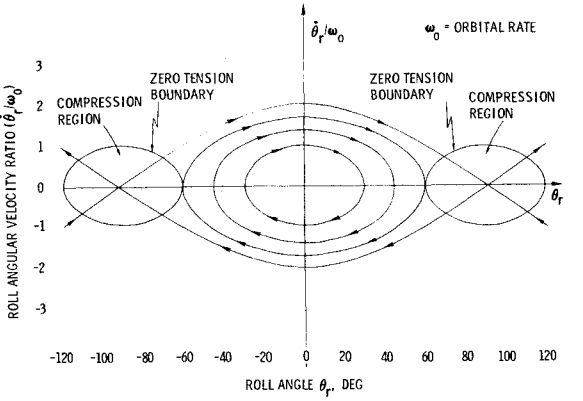

Fig. 4 Roll phase-plane diagram.

to maximum tension) is when $\theta_{rm}=0$ and it is zero when $\theta_{rm}=60$ deg. For $\theta_{rm}>60$ deg the array is in compression. The tension for a dumbbell with end masses M_{ant} is given by the equation

$$F=T(L\omega_0^2/2)M_{ant} \tag{3}$$

which is equivalent to Eq.(1) when $\sigma=\theta_r=\dot{\theta}_r=0$.

IV. Phase-Plane Analysis

The relationship between the roll angle and the roll rate can be obtained from the integration of the roll restoring angular acceleration expression

$$\ddot{\theta}_r=-2\omega_0^2\sin 2\theta_r \tag{4}$$

Multiplying Eq. (4) by $\dot{\theta}_r$ and integrating one obtains

$$\dot{\theta}_r^2/2=\omega_0^2\cos 2\theta_r+C \tag{5}$$

Closed trajectories in the phase plane $\dot{\theta}_r$ vs θ_r are separated from the unterminating ones by the solution of Eq. (5) which passes through $\theta_r=90$ deg, $\dot{\theta}_r=0$. For this solution, Eq. (5) is

$$(\dot{\theta}_r/\omega_0)^2=2(1+\cos 2\theta_r) \tag{6}$$

which is plotted in Fig. 4 along with other solutions corresponding to different initial values of $\dot{\theta}_r$ and θ_r. Also plotted is the case $T=0$ in Eq. (2) which delineates a region of compression in the $\dot{\theta}_r$, θ_r plane. These results show that the maximum roll angle must be less that 60 deg and should preferably be no greater than 30 deg. For the latter case the maximum tension will be 2/3 that at $\theta_{rm}=0$.

V. Flexibility Effects

The flexibility characteristics (natural frequencies and mode shapes) of the array play an important role in the design of the system. An insight into the nature of the normal modes can be obtained by examining those for a cable with and without tip masses. In general, the pitch and roll (in- and out-of-plane, respectively) librational modes are straight with 1.73 ω_0 and $2\omega_0$ frequencies in the linear range, respectively. The addition of a tip mass tends to increase the natural frequencies of all higher order modes.[4] It may thus be concluded that the array should maintain a straight (linear) configuration in a rolling librational mode up to 30 deg maximum angle.

VI. Summary and Conclusions

A concept for a gravitationally stabilized satellite solar power station in orbit has been described. The system consists of an array of solar cells feeding electric energy to a microwave antenna at the end of an Earth-pointing cable. Received power at the ground is in the 5000 to 10,000 MW range. The principal advantages of this concept are that 1) no excessively large structural subassemblies are required and 2) passive, long-life attitude control for the array is used. This concept separates the conventional very large solar flux collection assemblies into individual segments mutually connected by a gravitationally stabilized power distribution cable. Other desirable characteristics of the system are a gravitationally induced tension in the array and quite substantial restoring torques about the pitch and the roll axes. Rolling motion prevents the mutual shading of the array elements at the equinoxes.

Further studies to optimize the system parameters such as the size, shape, mass, and power are required, however, to more fully assess the feasibility and cost effectiveness of this concept.

References

[1]P.E. Glaser, "Evolution of the Satellite Solar Power Station (SSPS) Concept," *Journal of Spacecraft and Rockets*, Vol. 13, Sept. 1976. pp. 573-576.

[2]P.E. Glaser et al, "Feasibility Study of a Satellite Solar Power Station," NASA CR-2357, Feb. 1974.

[3]ECON Inc., "Space-Based Solar Power Conversion and Delivery Systems Study," Report No. 76-145-IB, March 31, 1976.

[4]G.B. Andeen, "Orbital, Attitude, and Deployment Considerations for a Passive Space Array," Stanford Research Institute Report No. 5, Dec. 1975.

Simple Algorithm for Intersecting Two Conical Surfaces

Carl Grubin*
Northrop Corporation, Hawthorne, Calif.

A PROBLEM of recurring interest in space mechanics is determining the intersection of two conical surfaces. For example, measuring the angle between a known star reference and an unknown vector locates the vector on a cone whose axis is the star line and whose semivertex angle is the measured angle. A second simultaneous measurement using another star locates the vector on a second cone. Obviously the vector lies at the intersection(s) of the two cones. This paper develops a simple algorithm for determining the intersection.

Analysis

Designate unit vectors along the cone axes as $\bar{e}_1$, $\bar{e}_2$, respectively. The angles between $\bar{e}_1$, $\bar{e}_2$ and the unknown

Received Nov. 11, 1976; revision received Nov. 29, 1976.
Index categories: Spacecraft Attitude Dynamics and Control; Spacecraft Navigation, Guidance, and Flight-Path Control Systems.

*Engineering Specialist, Electronics Division. Associate Fellow AIAA.